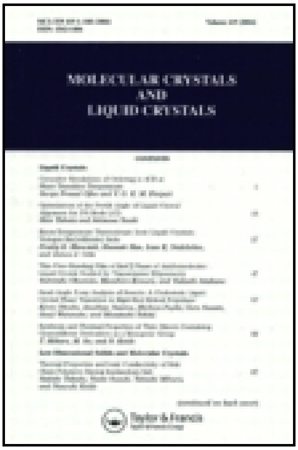

Molecular Crystals and Liquid Crystals
Publication details, including instructions for authors and subscription information:
http://www.tandfonline.com/loi/gmcl20

# Vibrational and Electronic Properties of Perylenediimide Linked to Fullerene and Tetrathiafulvalene

Andrzej Łapiński [a] , Andrzej Graja [a] , Iwona Olejniczak [a] , Andrzej Bogucki [a] , Maria Połomska [a] , Jérôme Baffreau [b] , Lara Perrin [b] , Stéphanie Leroy-Lhez [b] & Piétrick Hudhomme [b]

[a] Institute of Molecular Physics, Polish Academy of Sciences, Poznań, Poland

[b] Laboratoire de Chimie, Ingénierie Moléculaire et Matériaux d'Angers, UMR CNRS, Université d'Angers, Angers, France

Version of record first published: 23 Aug 2006

To cite this article: Andrzej Łapiński, Andrzej Graja, Iwona Olejniczak, Andrzej Bogucki, Maria Połomska, Jérôme Baffreau, Lara Perrin, Stéphanie Leroy-Lhez & Piétrick Hudhomme (2006): Vibrational and Electronic Properties of Perylenediimide Linked to Fullerene and Tetrathiafulvalene, Molecular Crystals and Liquid Crystals, 447:1, 87/[405]-103/[421]

To link to this article: http://dx.doi.org/10.1080/15421400500385381

*Mol. Cryst. Liq. Cryst.*, Vol. 447, pp. 87/[405]–103/[421], 2006
Copyright © Taylor & Francis Group, LLC
ISSN: 1542-1406 print/1563-5287 online
DOI: 10.1080/15421400500385381

Taylor & Francis
Taylor & Francis Group

# Vibrational and Electronic Properties of Perylenediimide Linked to Fullerene and Tetrathiafulvalene

**Andrzej Łapiński**
**Andrzej Graja**
**Iwona Olejniczak**
**Andrzej Bogucki**
**Maria Połomska**
Institute of Molecular Physics, Polish Academy of Sciences,
Poznań, Poland

**Jérôme Baffreau**
**Lara Perrin**
**Stéphanie Leroy-Lhez**
**Piétrick Hudhomme**
Laboratoire de Chimie, Ingénierie Moléculaire et Matériaux d'Angers,
UMR CNRS, Université d'Angers, Angers, France

*Solid-state electronic (UV-Vis) and vibrational (IR) spectra of the tetrathiafulvalene-perylenediimide (PDI-TTF) 1 and perylenediimide-fullerene (PDI-$C_{60}$)* ***2*** *dyads as well as PDI* ***3****, TTF* ***8*** *and fullerene* ***9*** *derivatives used as references molecules were investigated in the frequency range between 400 and 45,500 cm$^{-1}$. Electronic and vibrational features of the dyads were compared and analysed. Molecular geometry of the compounds and their IR and Raman theoretical spectra were calculated. It was stated, that small redistribution of the charges occurs in both moieties of these dyads. This effect is observed as shifts of both electronic and vibrational bands of the dyads in comparison with the respective bands of free components.*

**Keywords:** electronic spectra; normal modes analysis; perylenediimide-fullerene dyad; perylenediimide-tetrathiafulvalene dyad; vibrational spectra

This research was undertaken as part of the European collaborative COST Program (Action D14/0004/99). We thank BASF-AG, Ludwigshafen, for providing starting material 1,6,7,12-tetrachloroperylenetetracarboxylic dianhydride.

Address correspondence to Andrzej Graja, Institute of Molecular Physics, Polish Academy of Sciences, PL 60-179 Poznań, Poland.

## INTRODUCTION

Historically applied for industrial purposes as pigments due to their insolubility and photostability [1], perylene-3,4,9,10-tetracarboxydiimides (PDI) belong now to the most fascinating functional molecular materials [2]. These are potentially interesting electron-accepting materials and the best n-type molecular semi-conductors available to date, providing promising compounds for application in electronic devices. New developments in the field of PDI-based functional materials are now devoted towards the synthesis of donor – PDI molecular assemblies with the aim of promoting an efficient photoinduced electron transfer reaction between these two redox active units and long-lived charge-separated states. Several approaches for designing and creating donor-$\sigma$-acceptor (D-$\sigma$-A) dyads have been recently proposed for applications in molecular electronics as switches, wires or rectifiers, in the development of artificial photosynthetic systems or efficient photovoltaic devices [3]. Thus PDI derivatives have been associated to different donors such as zinc porphyrin [4], pyrene [5], ferrocene [6] or oligo(*p*-phenylenevinylene) [7]. PDI was very recently linked to fullerene $C_{60}$ with the aim of inducing an intramolecular energy transfer and to play the role of light-harvesting antenna for enhancing the efficiency of organic solar cells [8–10]. To our knowledge, this acceptor has never been associated in a dyad system with tetrathiafulvalene (TTF) as the donor counterpart.

We have been interested in the development of a dissymmetrical perylene-3,4,9,10-tetracarboxydiimide building block in order to investigate its grafting to both tetrathiafulvalene and $C_{60}$ to obtain PDI-TTF and PDI-$C_{60}$ dyads **1** and **2**, respectively. The main aim of this work is to provide information on electronic and vibrational properties of these two PDI dyads with an electron donor molecule (TTF-based **8**) and an electron acceptor molecule (modified $C_{60}$ **9**). The molecular geometry and dynamics of these adducts are simulated and theoretical IR and Raman spectra are compared with the experimental data. Our overall goal is to study the correlation between the structure of new chromophoric systems and their electron and vibrational features, deduced from spectral response in a broad frequency range.

## EXPERIMENTAL

Compounds chosen for spectral investigations, i.e., PDI-TTF **1** and PDI-$C_{60}$ **2** dyads as well as reference molecules (PDI **3**, modified TTF **8** and modified $C_{60}$ **9**) are shown in Scheme 1.

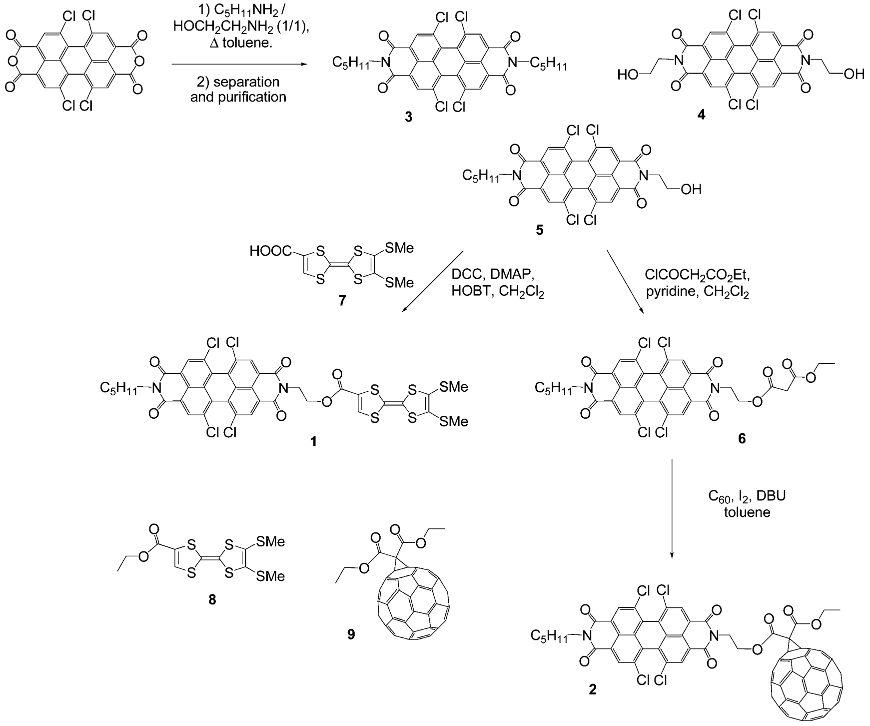

**SCHEME 1** Synthesis and chemical structure of the investigated samples: the dyad **1** (PDI-TTF), the dyad **2** (PDI-$C_{60}$), as well as the reference molecules of the PDI **3**, the modified TTF **8**, and the modified $C_{60}$ **9**.

The readily-available dissymmetrical PDI **5** tetrasubstituted at the bay region by chlorine atoms was obtained by direct condensation of 1-pentylamine and 2-aminoethanol in stoichiometric ratio on 1,6,7,12-tetrachloroperylene tetracarboxylic dianhydride in refluxing toluene. After separation from both symmetrical PDI derivatives **3** and **4**, dissymmetrical monoalcohol **5** was isolated in 28% yield. PDI-TTF dyad **1** was then synthesized in a one-pot esterification reaction, which was cleanly carried out by using TTF monoacid **7** [11] and PDI monoalcohol **5** in the presence of DCC as an activating reagent and both DMAP and HOBT to afford dyad **1** [12] in 94% yield. Using the same peptide coupling conditions for the reaction between TTF monoacid **7** and ethanol, TTF **8** was synthesized as the reference for further studies.

Methanofullerene dyad **2** was obtained using a two-step strategy by successive transformation to the corresponding malonate using ethyl malonyl chloride and further cyclopropanation with iodine and DBU [13]. Purification by silica gel column chromatography ($CH_2Cl_2$/EtOAc 4/1 as the eluents) afforded dyad **2** [14] in 41% yield. Reference compound **9** was efficiently prepared according to the Bingel's methodology starting from α-bromoethyl malonate [15].

Electronic absorption spectra in the range between 220 and 2500 nm were recorded with a Perkin Elmer UV-Vis-NIR Lambda 19 spectrometer, at room temperature. The spectra of powdered samples (**1–3**, **8**, **9**) were taken in KBr pellets containing dispersed compounds with weight concentrations 1:1000–1:8000, depending on the band intensities. Vibrational spectra in the range 400–7000 $cm^{-1}$ were also recorded with a FT-IR Bruker Equinox 55 spectrometer, in KBr pellets with a typical concentration 1:1000, at room temperature. Raman scattering of the light was investigated with a Bruker IFS 66 FRA 106 spectrometer (the exciting wavelength is $\lambda = 1.064\,\mu m$). We focused our attention on two spectral regions: the first between 220 and 600 nm (45500–17000 $cm^{-1}$), where the electronic excitations of the dyads are observed, and the second between 400 and 1800 $cm^{-1}$, where the intramolecular vibrations occur. Between these two regions, only weak absorption bands typical for C−H group vibrations are observed.

With the help of the Gaussian 03 program [16], we performed normal mode analysis for **1**, **3**, **8**, and **9**. The equilibrium geometry and vibrational modes of these neutral molecules were evaluated with a Becke-style 3-Parameter Density Functional Theory with the Lee-Yang-Parr correlation functional (B3LYP) using a basis set of 3-21G (**1** and **9**), 6-31G (**3**) or 6-311++G(d,p) (**8**). Moreover, the assignment of normal modes was proposed using the program GaussView.

## RESULTS AND DISCUSSION

### Electronic Spectra

The UV-Vis absorption spectra of investigated compounds **1–3**, **8**, **9** are shown in Figures 1a and b. In the modified fullerene **9**, two strong and overlapping optical absorption bands at 267 and 334 nm are observed (Fig. 1a). They correspond to the bands identified as the dipole-allowed transitions observed in prisstine $C_{60}$ at 266 and 343 nm, respectively [17]. The band at 334 nm undergoes a hypochromic shift by 9 nm compared to the wavelength of the respective band of $C_{60}$ but the other band is practically not shifted; both of the bands are broadened. The band centered at 334 nm is slightly more blue-shifted and broadened in the dyad **2**. Similar, but stronger shifts were

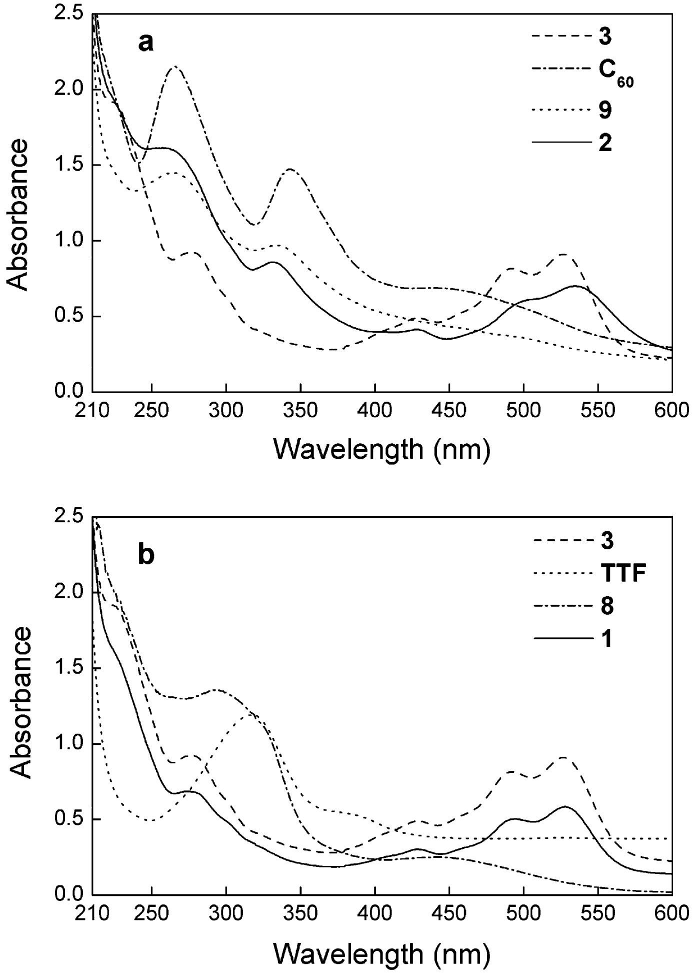

**FIGURE 1** Electronic absorption spectra of: (a) the dyad **2** (PDI-$C_{60}$), PDI **3**, the modified $C_{60}$ **9**, and fullerene $C_{60}$ (shown for comparison); (b) the dyad **1** (PDI-TTF), PDI **3**, the modified TTF **8**, and the tetrathiafulvalene TTF (shown for comparison).

observed in other fullerene adducts, e.g., in the *bis*-linked TTF-fullerene derivatives [18–20], *meso,meso*-linked oligoporphyrin bearing one or two fullerene moieties [21] and the fullerene-zinc porphyrin dyad [22]. Weaker electron donor properties of the perylenediimide **3** with the ionization potential slightly above I = +1.95 V, in comparison with TTF **8** (I = +0.63 V) cause a smaller bonding energy of the dyad **2**, and as a consequence – relatively small fullerene band shift.

The electronic absorption spectrum of the PDI **3** in KBr pellet (Fig. 1a) is dominated by typical perylene triple absorption with local maxima at 527, 493, and 458 nm; there are also weak bands at 429, 277, and 224 nm. The triple absorption characteristic for the highest occupied energy levels of perylene (dissolved in cyclohexane) shows maxima at 435, 408, and 387 nm but another bands are centered at 371, 252, and 245 nm [23]. The adequate triple absorption of all known PDIs in organic solvents is observed at about 526, 490, and 458 nm [24]. The weak dependence of the spectra on the terminal group in various PDIs is clear because the chromophore has nodes in the orbitals HOMO and LUMO at the nitrogen atoms [25]. Thus, according to our measurements in the solid state, **3** shows the typical electronic absorption for perylenediimides in organic solvents. Some of the bands of **3** can be identified in its dyad **2** with $C_{60}$. Doubtless, the bands at 535, 499, and 428 nm can be attributed to typical perylenediimide absorptions. Two former bands show bathochromic shift by a few nanometres (on an average 7 nm) with regard to components of the triple absorption of **3**. In opposite, the band at 428 nm is practically not shifted.

On the other hand, our earlier investigations on both porphyrin- and TTF-containing fullerene-derived adducts [18–22] showed, that the spectra of compounds derived from $C_{60}$, have some common features, virtually not dependent on the attached molecular groups. In spite of the covalent linkage and vicinity of both fullerene and TTF or porphyrin $\pi$-electron systems, the observed spectral effects can be mainly ascribed to through-bond interaction between the two moieties [20].

The electronic spectrum of TTF (Fig. 1b) contains a strong absorption band at 318 nm and much weaker absorption at about 380 nm. The spectrum of modified TTF molecule **8** is completely different: a broad, unsymmetrical absorption is observed between 280 and 345 nm and much weaker band is centered at 445 nm. This shows that modification of the TTF molecule changes distinctly its electronic structure. The spectrum of the dyad **1** consists of the bands at 528, 494, 429, about 275 and about 225 nm and it reproduces well the respective spectrum of **3**. It means that TTF does not change distinctly the electronic structure of the chromophore **3**. A similar effect was observed in the fullerene-tetrathiafulvalene cyclohexene fused polyads [18]: no band of TTF and weak influence of the bonding on the $C_{60}$ spectrum were observed. In opposite, it was stated that the fullerene absorption bands undergo distinct blue shifts strongly dependent on the number of substituent groups but weakly dependent on their nature [18,19,22].

## Vibrational Spectra

In order to analyze the experimental data of **1** and **2** dyads we recorded and calculated infrared absorption and Raman scattering spectra for the molecules **3**, **8**, and **9**. The spectra of the investigated compound **1** with its reference compounds **3** and **8** are presented in Figure 2.

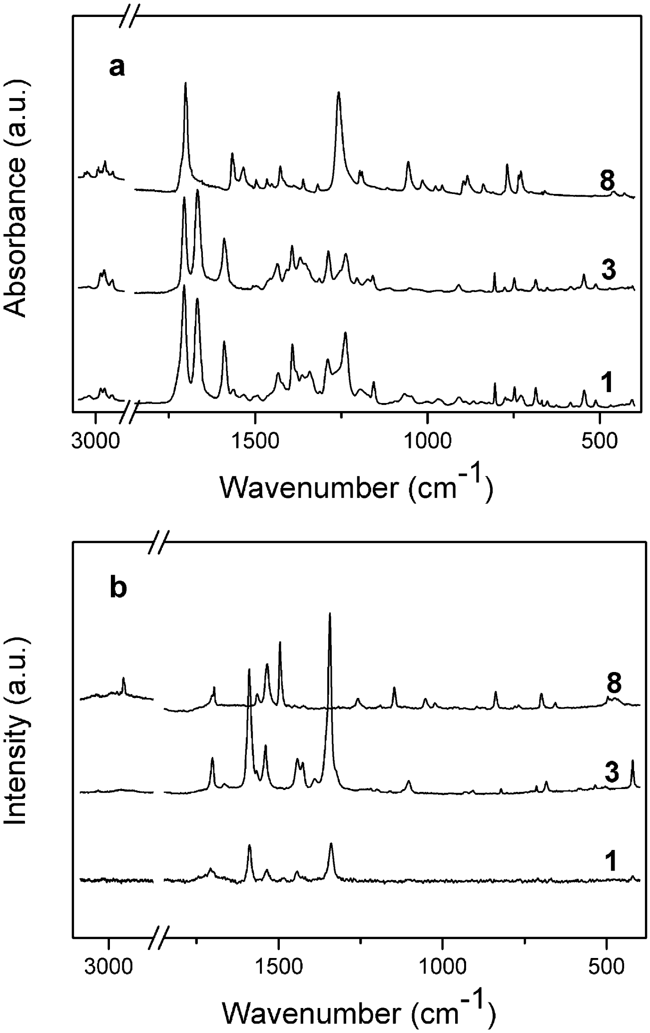

**FIGURE 2** IR absorption (a) and Raman (b) spectra of the dyad **1** (PDI-TTF), PDI **3**, and the modified TTF **8**.

Most of the bands attributed to vibrations of **3** can be found in the spectra of the dyad **1** at the same or slightly shifted frequencies. For example, the strongest bands of **3** at 420, (512), 546, 584, 653, 686, (728), 748, 776, 806, 910, 1104, 1237, 1287, 1341, (1392), 1589, 1667, (1705), (2928), and (2957) $\mathrm{cm}^{-1}$ (the wavenumbers of the bands which coincide with the bands of **8** are given in parentheses) have their counterpart in **1** at 422, 512, 546, 585, 652, 686, 728, 748, 775, 804, 908, 1107, 1238, 1289, 1341, 1391, 1589, 1668, 1706, 2923, and 2956 $\mathrm{cm}^{-1}$ (for other coinciding bands see Table 1). The vibrational spectra of the dyad **2** with its reference molecules **3** and **9** are shown in Figure 3. Similarly, many bands attributed to vibrations of **3** can also be found in the spectra of the compound **2** at almost the same position. For example, the strongest bands of **3** at 420, 546, (584), 653, 748, 776, 806, 910, 1104, (1237), (1287), 1341, 1392, 1589, 1667, 1705, (2928), and (2957) $\mathrm{cm}^{-1}$ (the wavenumbers of the bands which coincide with the bands of **9** are given in parentheses) have their counterpart in **2** at 419, 547, 582, 652, 747, 774, 804, 909, 1095, 1235, 1288, 1342, 1390, 1588, 1667, 1705, 2928, and 2953 $\mathrm{cm}^{-1}$. The bands related only to **9** observed at 258, 272, 287, 430, 445, 486, 531, 551, 704, 841, 1020, 1060, 1178, 1266, 1428, 1463, and 1745 $\mathrm{cm}^{-1}$ have their counterpart in **2** at 257, 269, 287, 429, 442, 484, 531, 551, 704, 841, 1020, 1062, 1176, 1266, 1431, 1462, and 1746 $\mathrm{cm}^{-1}$ (for other coinciding bands see Table 2). Therefore, we propose the assignment of the vibrational bands for **1** and **2** dyads following the analysis of **3**, **8**, and **9** reference molecules.

The normal mode assignment for dyads have been proposed based on the comparison of calculated and experimental vibrational spectra; detailed computer output is available upon request. Because of the large number of normal modes (84 atoms and 246 modes for **1**, and 134 atoms and 396 modes for **2**), this assignment is based on comparison of simulated and experimental spectral peaks rather than on individual modes. Positions of well separated bands, multiplets and their shape were taken into consideration. Moreover, the description of the modes presented in the Tables 1 and 2 has been verified using standard GaussView program base on the dynamic displacement visualization.

We started our detailed investigations of IR and Raman spectra of **3**, **8**, **9** compounds from an analysis of possible conformations. For **3** we have taken into account two different conformations: one adopts a boat conformation with two pentyl groups upward from the PDI plane (point group is $C_s$), the other a chair conformation where one pentyl group is upward, the other one is downward (point group is $C_{2h}$). For such conformers of **3** with $C_{2h}$ and $C_s$ symmetry, the calculated frequencies of normal modes at B3LYP level of theory were

**TABLE 1** Normal Mode Analysis of **1** Based on the Experimental and Calculated Spectra of **3** and **8**

| Experiment (cm$^{-1}$) | | | | | | Calculation (cm$^{-1}$) | | Approximate description$^{c}$ |
|---|---|---|---|---|---|---|---|---|
| **1** | | **3** | | **8** | | | | |
| IR | Raman | IR | Raman | IR | Raman | **3**$^{a}$ | **8**$^{b}$ | |
| 3096 | | 3100 | | 3096 | | 3255 | 3227 | C–H str., in **3**; C–H str., in **8** |
| 3057 | | 3063 | 3060 | | | 3172 | | C–H str., pentyl groups in **3** |
| 2956 | | 2957 | | 2954 | 2954 | 3115 | 3138 | C–H str., pentyl groups in **3**; C–H str., methyl groups in **8** |
| 2923 | | 2928 | 2931 | 2920 | 2919 | 3097 | 3050 | C–H str., pentyl groups in **3**; C–H str., methyl groups in **8** |
| 2867 | | 2869 | 2870 | | | 3037 | | C–H str., pentyl groups in **3** |
| 2857 | | 2856 | | 2853 | | 3026 | 3037 | C–H str., pentyl groups in **3**; C–H str., ethyl groups in **8** |
| 1706 | 1707 | 1705 | 1702 | 1701 | 1700 | 1694 | 1753 | C=O str., in **3**; C=O str., in **8** |
| 1668 | 1664 | 1667 | 1665 | | | 1655 | | C=O str., in **3** |
| 1589 | 1588 | 1589 | 1589 | | | 1624 | | C=C str., C=O str., in **3** |
| 1562 | 1561 | 1559 | 1567 | 1566 | 1565 | 1614 | 1610 | C=C str., C=O str., in **3**; C=C str., in **8** |
| 1534 | 1535 | | | 1534 | 1534 | | 1582 | C=C str., in **8** |
| 1492 | 1484 | 1496 | 1495 | 1497 | 1495 | 1548 | 1529 | C–H bend., CC str., in **3**; C=C str., in **8** |
| 1433 | 1442 | 1435 | 1443 | 1427 | 1450 | 1484 | 1481 | H–C–H bend., pentyl groups in **3**; C–H bend., str., in **3**; H–C–H bend., methyl groups in **8** |
| 1391 | | 1392 | 1390 | 1387 | | 1441 | 1399 | H–C–H wag., pentyl groups in **3**; C–H bend., H–C–H bend., ethyl groups in **8** |
| 1364 | | | | 1360 | | | 1355 | H–C–H bend., methyl groups in **8** |
| 1341 | 1339 | 1341 | 1343 | | | 1376 | | CC str., in **3** |
| 1312 | | 1314 | | 1318 | | 1315 | 1298 | H–C–H wag., pentyl groups in **3**; C–H bend., H–C–H tw., ethyl groups in **8**; |

(*Continued*)

**TABLE 1** Continued

| Experiment ($cm^{-1}$) | | | | | | Calculation ($cm^{-1}$) | | |
|---|---|---|---|---|---|---|---|---|
| **1** | | **3** | | **8** | | | | Approximate description[c] |
| IR | Raman | IR | Raman | IR | Raman | **3**[a] | **8**[b] | |
| 1289 | | 1287 | | | | 1285 | | H–C–H tw., pentyl groups in **3**; CC str., in **3** |
| 1238 | | 1237 | | | | 1263 | | C–H bend., CC def., in **3** |
| 1156 | | 1159 | 1160 | | | 1157 | | C–C def., pentyl groups in **3** |
| | 1107 | | 1104 | | | 1126 | | C–H bend., CC def., in **3** |
| 970 | | 967 | | 958 | | 973 | 993 | C–H bend., in **3**; C–H def., methyl groups in **8** |
| 908 | | 910 | 908 | | | 911 | | C–C def., pentyl groups in **3** |
| 867 | | 869 | 867 | | | 876 | | CC def., in **3** |
| 804 | | 806 | 804 | | | 808 | | CC def., in **3** |
| 775 | | 776 | | | | 780 | | CC def., in **3** |
| | 767 | | | | 767 | | 764 | C-S str., in **8** |
| 748 | | 748 | 744 | | | 752 | | CC def., in **3** |
| 728 | | 728 | 729 | 729 | 730 | 721 | 741 | CC def., in **3**; C–S str., in **8** |
| 703 | 709 | | | 700 | 699 | | 680 | C–S str., in **8** |
| 686 | | 686 | 684 | | | 678 | | CC def., in **3** |
| 668 | 669 | 671 | 671 | 668 | 657 | 652 | 677 | CC def., in **3**; C–S str., in **8** |
| 652 | | 653 | | | | 624 | | C–C def., C=C def., in **3** |
| 626 | | 627 | | | | 593 | | CC def., in **3** |
| 617 | | 615 | | 618 | | | 552 | C–S def., in **8** |
| 585 | | 584 | 585 | | | 569 | | CC def., in **3** |
| 568 | | 563 | | | | 552 | | CC def., in **3** |
| 546 | | 546 | 548 | | | 529 | | CC def., in **3** |
| 512 | | 512 | | 514 | | | 530 | C–S def., in **8** |
| 422 | 420 | 420 | 420 | | | 416 | | CC def., in **3** |
| 406 | | 406 | | | | 363 | | CC def., in **3** |

[a] B3LYP/6-31G (unscaled).

[b] B3LYP/6-311++G(d,p) (unscaled).

[c] Approximate mode description: str = stretching, bend = bending, def = deformation, tw = twisting, wag = wagging.

obtained almost at the same position. Moreover, the total energy for the “boat” and “chair” conformation is also very similar: E(boat) = −3562,01855 hartrees and E(chair) = −3562.01873 hartrees. It can

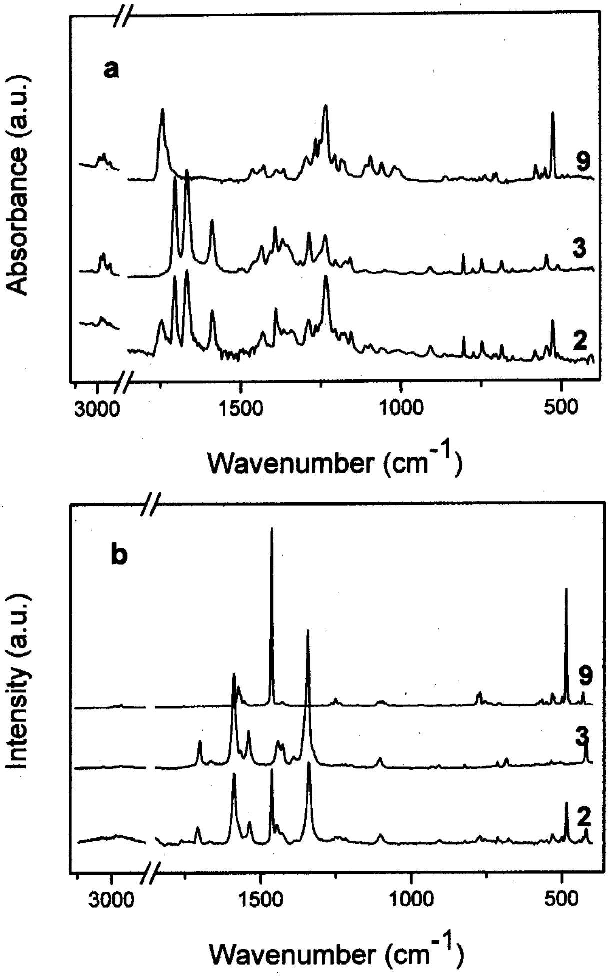

**FIGURE 3** IR absorption (a) and Raman (b) spectra of the dyad **2** (PDI-$C_{60}$), PDI **3**, and the modified $C_{60}$ **9**.

suggest that the conformation of pentyl groups does not strongly influence the spectrum. Presumably these groups do not interact with the core of the molecule **3** and hence do not significantly influence its optical activity. Middle part of **3** in optimized structure is not flat; the four chlorine atoms at the bay region are out of plane. In the case of compound **8** we have taken into account an arrangement of methyl groups. As a starting point in the optimization process, we considered many possible conformations of molecule **8**. We observed that the fully

**TABLE 2** Normal Mode Analysis of **2** Based on the Experimental and Calculated Spectra of **3** and **9**

| Experiment ($cm^{-1}$) | | | | | | Calculation ($cm^{-1}$) | | | Approximate description[d] |
|---|---|---|---|---|---|---|---|---|---|
| **2** | | **3** | | **9** | | | | | |
| IR | Raman | IR | Raman | IR | Raman | $C_{60}$[a] | 3[b] | 9[c] | |
| 3098 | | 3100 | | | | | 3255 | | C–H str., in **3** |
| 3068 | | 3063 | 3060 | | | | 3172 | | C–H str., pentyl groups in **3** |
| 2953 | 2968 | 2957 | | 2956 | 2956 | | 3115 | 3138 | C–H str., pentyl groups in **3**; C–H bend., ethylene groups in **9** |
| 2928 | 2923 | 2928 | 2931 | 2922 | 2929 | | 3097 | 3106 | C–H str., pentyl groups in **3**; H–C–H rck, ethylene groups in **9** |
| 2866 | 2864 | 2869 | 2870 | | | | 3037 | | C–H str., pentyl groups in **3** |
| 2854 | 2850 | 2856 | | 2852 | 2860 | | 3025 | 3071 | C–H str., pentyl groups in **3**; C–H rck, ethylene groups in **9** |
| 1746 | | | | 1745 | | | | 1733 | linkage def., in **9** |
| 1706 | 1708 | 1705 | 1702 | | | | 1694 | | C=O str., in **3** |
| 1667 | 1662 | 1667 | 1665 | | | | 1655 | | C=O str., in **3** |
| 1588 | 1589 | 1589 | 1589 | | | | 1624 | | C=C str., C=O str., in **3** |
| | 1537 | | | 1539 | | | 1570 | | CC str., in **3** |
| 1462 | 1463 | | | 1463 | 1464 | 1470 | | 1494 | $C_{60}$ def., in **9** |
| | 1445 | 1435 | 1443 | | | | 1484 | | H–C–H bend., pentyl groups in **3**; C–H bend., CC str., in **3** |
| 1431 | 1424 | | | 1428 | 1427 | 1429 | | 1448 | $C_{60}$ def., in **9** |
| 1390 | 1389 | 1392 | 1390 | | | | 1441 | | H–C–H wag., pentyl groups in **3**; C–H bend., in **3** |
| 1365 | | | | 1366 | | | | 1353 | H–C–H tw., ethylene groups in **9** |
| 1342 | 1340 | 1341 | 1344 | | | | 1376 | | CC str., in **3** |
| 1288 | | 1287 | | 1296 | | 1290 | 1285 | 1307 | H–C–H tw., pentyl groups in **3**; CC str., in **3**; $C_{60}$ def., in **9** |
| 1266 | | | | 1266 | | 1260 | | 1274 | $C_{60}$ def., in **9** |

*(Continued)*

**TABLE 2** Continued

| Experiment ($cm^{-1}$) | | | | | | Calculation ($cm^{-1}$) | | | Approximate description[d] |
|---|---|---|---|---|---|---|---|---|---|
| **2** | | **3** | | **9** | | | | | |
| IR | Raman | IR | Raman | IR | Raman | $C_{60}$[a] | 3[b] | 9[c] | |
| 1253 | 1249 | | | 1252 | 1251 | 1251 | | 1252 | $C_{60}$ def., linkage def., in **9** |
| 1235 | 1236 | 1237 | | 1234 | 1238 | 1237 | 1263 | 1232 | C–H bend., CC def., in **3**; $C_{60}$def., in **9**; linkage def., in **9** |
| | 1218 | | 1218 | | | | 1213 | | C–H bend., CC def., in **3** |
| 1205 | | | | 1206 | | 1205 | | 1213 | $C_{60}$ def., linkage def., in **9** |
| 1186 | | | | 1186 | | 1182 | | 1187 | $C_{60}$ def., linkage def., in **9** |
| 1176 | | | | 1178 | | 1175 | | 1181 | $C_{60}$ def., in 9 |
| 1156 | | 1159 | 1160 | | | | 1157 | | C–C def., pentyl groups in **3** |
| 1111 | | | | 1110 | | 1115 | | 1108 | $C_{60}$ def., in **9** |
| 1095 | 1102 | | 1104 | | 1102 | 1101 | 1126 | 1092 | C–H bend., CC def., in **3**; $C_{60}$ def., linkage def., in **9** |
| 1062 | | | | 1060 | | 1061 | | 1056 | $C_{60}$ def., linkage def., in **9** |
| 1020 | | | | 1020 | | 1020 | | 1016 | $C_{60}$ def., linkage def., in **9** |
| 963 | | 967 | | | | | 973 | | C–H bend., in **3** |
| 909 | 905 | 910 | 908 | 912 | 906 | 911 | 911 | 933 | C–C def., pentyl groups in **3**; $C_{60}$ def., linkage def., in **9** |
| 865 | | 869 | 867 | 865 | | | 876 | 873 | CC def., in **3**; linkage def., in **9** |
| 841 | | | | 841 | | | | 840 | linkage def., in **9** |
| 822 | 821 | 823 | 822 | | | | 849 | | CC def., in **3** |
| 804 | | 806 | 804 | 806 | 808 | 796 | 808 | 795 | CC def., in **3**; $C_{60}$ def., linkage def., in **9** |
| 774 | 771 | 776 | | 771 | 771 | 775 | 780 | 781 | CC def., in **3**; $C_{60}$ def., linkage def., in **9** |
| 755 | 754 | | | 756 | 755 | 753 | | 755 | $C_{60}$ def., linkage def., in **9** |
| 747 | | 748 | | | | | 752 | | CC def., in **3** |

(*Continued*)

**TABLE 2** Continued

| Experiment ($cm^{-1}$) | | | | | | Calculation ($cm^{-1}$) | | | Approximate description[d] |
|---|---|---|---|---|---|---|---|---|---|
| **2** | | **3** | | **9** | | | | | |
| IR | Raman | IR | Raman | IR | Raman | $C_{60}$[a] | 3[b] | 9[c] | |
| 712 | 712 | | | 712 | 711 | 712 | | 719 | $C_{60}$ def., in **9** |
| 704 | | | | 704 | 704 | 709 | | 705 | $C_{60}$ def., in **9** |
| 672 | 676 | 671 | 671 | 672 | 672 | 668 | 678 | 669 | CC def., in **3**; $C_{60}$ def., in **9** |
| 652 | | 653 | | | | | 624 | | C−C def., C=C def., in **3** |
| 627 | | 627 | | | | | 593 | | CC def., in **3** |
| 582 | | 584 | 585 | 581 | 581 | 580 | 569 | 586 | CC def., in **3**; $C_{60}$ def., in **9**; |
| 575 | | | | 575 | 571 | 575 | | 574 | $C_{60}$ def., in **9** |
| 563 | 567 | | | 563 | 565 | 567 | | 564 | $C_{60}$ def., linkage def., in **9** |
| 558 | 551 | | | 557 | 551 | | | 554 | $C_{60}$ def., linkage def., in **9** |
| 547 | | 546 | 548 | | | | 529 | | CC def., in **3** |
| 527 | 531 | | | 527 | 531 | 526 | | 534 | $C_{60}$ def., in **9** |
| 498 | 499 | | | 498 | 498 | 497 | | 498 | $C_{60}$ def., linkage def., in **9** |
| 479 | 484 | | | 480 | 486 | 485 | | 485 | $C_{60}$ def., in **9** |
| | 442 | | | | 445 | | | 444 | $C_{60}$ def., linkage def., in **9** |
| | 429 | | | | 430 | 433 | | 431 | $C_{60}$ def., in **9** |
| | 419 | | 420 | | | | 416 | | CC def., in **3** |
| | 344 | | | | 334 | | | 322 | linkage def., in **9** |
| | 324 | | 324 | | | | 322 | | CC def., in **3** |
| | 287 | | | | 287 | | | 280 | linkage def., in **9** |
| | 269 | | | | 272 | 273 | | 276 | $C_{60}$ def., in **9** |
| | 257 | | | | 258 | | | 261 | $C_{60}$ def., in **9** |
| | 227 | | 222 | | | | 217 | | CC def., in **3** |

[a] IR and Raman data taken from [26].

[b] B3LYP/6-32G (unscaled).

[c] B3LYP/3-21G (unscaled).

[d] Approximate mode description: str = stretching, bend = bending, def = deformation, tw = twisting, wag = wagging, rck = rocking.

optimized geometry of **8** for DFT methods is slightly distorted from a plane to a boat conformation with methyl groups displaced from this plane to the same side. The normal modes calculation for **9** was carried out with $C_2$ symmetry.

The normal mode analysis for fully optimized **3**, **8**, and **9** molecules was performed using DFT(B3LYP) level of theory. Based on their normal modes dynamic visualization we could identify and describe bands (see Tables 1 and 2). For example, the IR bands related mostly to the vibrations of pentyl groups are observed for dyad **1** at 908, 1156, 1289, 1312, 1391, 1433, 2857, 2867, 2923, 2956, and 3057 $cm^{-1}$, whereas for dyad **2** at 909, 1156, 1288, 1390, 1445, 2854, 2866, 2928, 2953, and 3068 $cm^{-1}$. The vibrations which are due to the deformation of fullerene are observed at 269, 429, 479, 498, 527, 563, 575, 582, 672, 704, 712, 755, 774, 804, 909, 1020, 1062, 1095, 1111, 1176, 1186, 1205, 1235, 1253, 1266, 1288, 1431, and 1462 $cm^{-1}$. These frequencies related to $C_{60}$ are almost unchanged comparing with pristine $C_{60}$: 273, 433, 485, 497, 526, 567, 575, 580, 668, 709, 712, 753, 775, 796, 911, 1020, 1061, 1101, 1115, 1175, 1182, 1205, 1237, 1251, 1260, 1290, 1429, and 1470 $cm^{-1}$ [26]. Base on our vibrational investigation we can conclude that the frequencies of the vibrations related to **3**, **8**, **9** are only slightly changed upon formation of the dyads.

## CONCLUSION

In this paper we report the spectral properties of the recently synthesized dyads PDI-TTF (**1**) and PDI-$C_{60}$ (**2**), together with the analysis of electronic and vibrational features. According to our knowledge, for the first time PDI molecule has been associated in a dyad system with TTF as the donor counterpart. Based on the *ab initio* calculations, the normal modes analysis and interpretation of the vibrational spectra is presented. Moreover, the possible conformations of the component moieties of the dyads are discussed. The electronic and vibrational spectra of **2** suggest a small redistribution of charges on both fullerene and perylenediimide moieties. It was deduced from the small vibrational band shifts as well as the broadening and shifts of some $C_{60}$ and PDI electronic bands after dyad formation. In opposite to **2**, a charge redistribution on both part of the dyad **1** was almost undetectable by spectral methods.

## REFERENCES

[1] Zollinger, H. (2003). *Color Chemistry*, 3rd edition, VCH: Wheinheim.
[2] Wuerthner, F. (2004). Perylene bisimide dyes as versatile building blocks for functional supramolecular architectures. *Chem. Commun.*, 1564.
[3] Gust, D. & Moore, T. A. (1991). *Photoinduced Electron Transfer*, Springer: Berlin.
[4] van der Boom, T., Hayes, R. T., Zhao, Y., Bushard, P. J., Weiss, E. A., & Wasielewski, M. R. (2002). Charge transport in photofunctional nanoparticles

self-assembled from zinc 5,10,15,20-tetrakis(perylenediimide)porphyrin building blocks. *J. Am. Chem. Soc.*, *124*, 9582.

[5] Wescott, L. D. & Mattern, D. L. Donor-$\sigma$-acceptor molecules incorporating a nonadecyl-swallowtailed perylenediimide acceptor. *J. Org. Chem.*, *68*, 10058.

[6] Li, Y., Wang, N., He, X., Wang, S., Liu, H., Li, Y., Li, X., Zhuang, J., & Zhu, D. (2005). Synthesis and characterization of ferrocene-perylenetetracarboxylic diimide-fullerene triad. *Tetrahedron*, *61*, 1563.

[7] Neuteboom, E. E., Meskers, S. C. J., van Hal, P. A., van Duren, J. K. J., Meijer, E. W., Janssen, R. A. J., Dupin, H., Pourtois, G., Cornil, J., Lazzaroni, R., Brédas, J. L., & Beljonne, D. (2003). Alternating oligo(p-phenylene vinylene)-perylene bisimide copolymers: Synthesis, photophysics, and photovoltaic properties of a new class of donor-acceptor materials. *J. Am. Chem. Soc.*, *125*, 8625.

[8] Hua, J., Meng, F., Ding, F., Li, F., & Tian, H. (2004). Novel soluble and thermally-stable fullerene dyad containing perylene. *J. Mater. Chem.*, *14*, 1849.

[9] Gómez, R., Segura, J. L., & Martín, N. (2005). Highly efficient light-harvesting organofullerenes. *Org. Lett.*, *7*, 717.

[10] Baffreau, J., Perrin, L., Leroy-Lhez, S., & Hudhomme, P. (2005). Perylene-3, 4:9, 10-bis(dicarboximide) linked to [60]fullerene as a light-harvesting antenna. *Tetrahedron Lett.*, *46*, 4599.

[11] Devic, T., Avarvari, N., & Batail, P. (2004). A series of redox active, tetrathiafulvalene-based amidopyridines and bipyridines ligands: Syntheses, crystal structures, a radical cation salt and group 10 transition-metal complexes. *Chem. Eur. J.*, *10*, 3697.

[12] Selected data for dyad **1**: $^1$H NMR (500 MHz, CDCl$_3$): 8.68 and 8.70 (2 s, 4H), 7.30 (s, 1H), 4.60 (m, 4H), 4.20 (t, 2H), 2.37 and 2.40 (2 s, 6H), 1.80 (m, 2H), 1.40 (m, 4H), 0.95 (t, 3H); $^{13}$C NMR (125 MHz, CDCl$_3$): 162.3, 162.2, 159.0, 135.4, 135.3, 133.1, 133.0, 132.9, 132.8; 132.5, 131.4, 131.3, 128.9, 128.4, 127.8, 127.6, 127.5, 123.3, 123.2, 122.7, 112.7, 109.4, 63.0, 40.9, 39.3, 29.1, 27.7, 22.4, 19.2, 13.9; MS (MALDI-TOF): 964 (M$^+$).

[13] Nierengarten, J. F., Gramlich, V., Cardullo, F., & Diederich, F. (1996). Regio- and diastereoselective bisfunctionalization of C$_{60}$ and enantioselective synthesis of a C$_{60}$ derivative with a chiral addition pattern. *Angew. Chem. Int. Ed. Engl.*, *35*, 2101.

[14] $^1$H NMR (500 MHz, CDCl$_3$): 8.65 (s, 2H), 8.63 (s, 2H), 5.09 (br t, 1H), 4.92 (br t, 1H), 4.78 (dt, $J = 4.5$ and 12 Hz, 1H), 4.62 (dt, $J = 4.5$ and 12 Hz, 1H), 4.57 (q, 2H), 4.20 (t, 2H), 1.76 (br t, 2H), 1.51 (t, 3H), 1.43 (br t, 4H), 0.93 (t, 3H); 13 C NMR (125 MHz, CDCl$_3$): 163.80, 163.19, 162.25, 162.19, 145.11, 145.06, 145.03, 144.99, 144.96, 144.81, 144.66, 144.56, 144.51, 144.43, 144.41, 143.66, 142.89, 142.79, 142.76, 141.98, 141.50, 138.90, 135.59, 135.45, 133.43, 132.98, 128.89, 128.30, 123.39, 123.37, 123.22, 122.56, 77.57, 71.32, 71.31, 63.76, 63.56, 51.99, 40.98, 39.13, 29.15, 27.76, 22.41, 14.26, 13.98; MS (MALDI-TOF, dithranol): 1476 (M + 2H)$^+$

[15] Bingel, C. (1993). *Chem. Ber.*, *126*, 1957.

[16] Frisch, M. J., Trucks, G. W., Schlegel, H. B., Scuseria, G. E., Robb, M. A., Cheeseman, J. R., Montgomery, Jr. J. A., Vreven, T., Kudin, K. N., Burant, J. C., Millam, J. M., Iyengar, S. S., Tomasi, J., Barone, V., Mennucci, B., Cossi, M., Scalmani, G., Rega, N., Petersson, G. A., Nakatsuji, H., Hada, M., Ehara, M., Toyota, K., Fukuda, R., Hasegawa, J., Ishida, M., Nakajima, T., Honda, Y., Kitao, O., Nakai, H., Klene, M., Li, X., Knox, J. E., Hratchian, H. P., Cross, J. B., Adamo, C., Jaramillo, J., Gomperts, R., Stratmann, R. E., Yazyev, O., Austin, A. J., Cammi, R., Pomelli, C., Ochterski, J. W., Ayala, P. Y., Morokuma, K., Voth, G. A., Salvador, P., Dannenberg, J. J., Zakrzewski, V. G., Dapprich, S., Daniels, A. D., Strain, M. C., Farkas, O., Malick, D. K., Rabuck, A. D., Raghavachari, K., Foresman, J. B., Ortiz, J. V., Cui, Q., Baboul, A. G., Clifford, S., Cioslowski, J., Stefanov, B. B., Liu, G., Liashenko, A., Piskorz, P.,

Komaromi, I., Martin, R. L., Fox, D. J., Keith, T., Al-Laham, M. A., Peng, C. Y., Nanayakkara, A., Challacombe, M., Gill, P. M. W., Johnson, B., Chen, W., Wong, M. W., Gonzalez, C., & Pople, J. A. (2003). *Gaussian 03*, Gaussian, Inc.: Pittsburgh, PA.

[17] Leach, S., Vervloet, M., Desprès, A., Brèheret, E., Hare, J. P., Dennis, T. J., Kroto, H. W., Taylor, R., & Walton, D. R. M. (1992). Electronic spectra and transitions of the fullerene $C_{60}$. *Chem. Phys.*, *160*, 451.

[18] Olejniczak, I., Graja, A., Bogucki, A., Golub, M., Hudhomme, P., Gorgues, A., Kreher, D., & Cariou, M. (2002). Vibrational and electronic properties of [60] fullerene-tetrathiafulvalenes (TTFs) cyclohexene fused polyads. *Synth. Met.*, *126*, 263.

[19] Olejniczak, I., Graja, A., Bogucki, A., Hudhomme, P., Gorgues, A., Kreher, D., & Cariou, M. (2002). New *bis*-linked tetrarhiafulvalenes (TTFs) to [60]fullerene: Spectral investigations. *Polish. J. Chem.*, *76*, 95.

[20] Olejniczak, I., Bogucki, A., Golub, M., Graja, A., Kreher, D., Cariou, M., Gorgues, A., & Hudhomme, P. (2002). Spectral studies of the *bis*-linked tetrathiafulvalenes (TTFs) to [60]fullerene. *Full Nanotubes & Carb. Nanostructures*, *10*, 117.

[21] Graja, A., Olejniczak, I., Bogucki, A., Bonifazi, D., & Diederich, F. (2004). Chromophoric interactions in [60]fullerene-porphyrin dyads investigated by solid-state UV-Vis and IR spectroscopies. *Chem. Phys.*, *300*, 227.

[22] Łapiński, A., Graja, A., Olejniczak, I., Bogucki, A., & Imahori, H. (2004). Supramolecular porphyrin/fullerene interactions studiem by spectra methods. *Chem. Phys.*, *305*, 277.

[23] Berlman, I. B., (1965). *Handbook of Fluorescence Spectra of Aromatic Molecules*, Academic Press: New York.

[24] Icli, S., Demiç, S., Dindar, B., Doroshenko, A. O., & Timur, C. (2000). Photophysical and photochemical properties of a water-soluble perylene diimide derivative. *J. Photochem. & Photobiol. A: Chem.*, *136*, 15.

[25] Langhals, H., Demmig, S., & Huber, H. (1988). Rotational barriers in perylene fluorescent dyes. *Spectrochim. Acta.*, *44A*, 1189.

[26] Martin, M. C., Du, X., Kwon, J., & Mihaly, L. (1994). Observation and assignment of silent and higher-order vibrations in the infrared transmission of $C_{60}$ crystals. *Phys. Rev. B*, *50*, 173.